

The Sensitivity Analysis on GNSS-R Soil Moisture Retrieval

Original

The Sensitivity Analysis on GNSS-R Soil Moisture Retrieval / Jia, Yan; Jin, Shuanggen; Yan, Qingyun; Savi, Patrizia. - ELETTRONICO. - (2021), pp. 2307-2311. (Intervento presentato al convegno 2021 Photonics & Electromagnetics Research Symposium (PIERS) tenutosi a Hangzhou, China nel 21-25 Nov. 2021) [10.1109/PIERS53385.2021.9694804].

Availability:

This version is available at: 11583/2955132 since: 2022-02-21T10:04:32Z

Publisher:

IEEE

Published

DOI:10.1109/PIERS53385.2021.9694804

Terms of use:

This article is made available under terms and conditions as specified in the corresponding bibliographic description in the repository

Publisher copyright

IEEE postprint/Author's Accepted Manuscript

©2021 IEEE. Personal use of this material is permitted. Permission from IEEE must be obtained for all other uses, in any current or future media, including reprinting/republishing this material for advertising or promotional purposes, creating new collecting works, for resale or lists, or reuse of any copyrighted component of this work in other works.

(Article begins on next page)

The sensitivity analysis on GNSS-R soil moisture retrieval

Yan Jia¹, Shuanggen Jin^{2,3}, Qingyun Yan³ and Patrizia Savi⁴

¹Department of Surveying and Geoinformatics, Nanjing University of Posts and Telecommunications Nanjing 210023, China

² Shanghai Astronomical Observatory, Chinese Academy of Sciences, Shanghai 200030, China

³ School of Remote Sensing and Geomatics Engineering, Nanjing University of Information Science and Technology, Nanjing 210044, China

⁴ Department of Electronics and Telecommunications, Politecnico di Torino, 10129 Torino, Italy

Abstract—The use of bistatic reflected global navigation satellite system (GNSS) signals as a means of sensing the Earth's surface is attracting widespread interest. It has the advantages of non-contact, large coverage area, and real-time which have attracted much attention during recent years. These reflected signals contain the information of the reflecting surface and therefore were applied to investigate the properties of the observed object, such as soil moisture (SM). Machine learning (ML) methods are featured with flexibility and are good at handling non-linear problems, modeling complex interactions between inputs and outputs, and have been rise attention for the GNSS-R SM retrieval field. The contribution of different input variables to SM is quite significant for optimizing the ML-based SM retrieval. In this paper, the typical random forest (RF) algorithm was adopted to evaluate the weight of input variables for ML-based SM retrieval. A simulation data set was built for training RF models, since the simulated data provide sufficient samples and show a more accurate relationship between the inputs and outputs. The SM predictions made by the RF methods are evaluated and compared with the simulation data set. The results show the contribution of a single variable to soil moisture retrieval, which can help with the ML-based GNSS-R SM retrieval to overcome the complex auxiliary variable problem.

1. INTRODUCTION

Soil moisture is a key component of the water cycle. It directly influences the amount of evaporation, infiltration, runoff, and the amount of water uptake by plants. Soil moisture creates energy fluxes between the land and the atmosphere, which impacts weather systems and may affect largely populated areas [1-5]. Moreover, the accurate monitoring of soil moisture serves as a factor in hydrological and vegetation monitoring and for better seasonal forecasting [6-7].

In recent years, GNSS-R as an Earth's surface remote sensing tool has been widely studied for various applications. Soil dielectric constant and soil moisture retrieval have started to produce some results. More recently, GNSS-R SM retrieval using an ML-based algorithm has generated considerable recent research interest [8-9].

2. METHODS

GNSS-Reflectometry is a form of a bistatic radar, which means the receiver and the transmitter have a considerable distance. Not like the most common type of monostatic radar that refers to the transmitter and the receiver are in the same place. The geometry of the monostatic radar determines that the transmitted signal will reflect along the same path, also known as backscattering. The non-nadir monostatic radar for surface remote sensing is most sensitive to surface roughness. For example, in a smooth surface, the reflected energy would forward to another path at an angle to the surface normal which is equal to the incident angle, and the transmitter gets no energy back. This is the main distinction to be considered between monostatic radar and bistatic radar in surface remote sensing [10].

GNSS-R geometry as a bistatic radar sensing surface is shown in Fig. 1 [11-15]. The transmitter GPS satellite and the receiver are all above the surface, and the scattering happens in the regions around the specular point. The specular point is defined as a reflection point that the incident and reflected angles are equal. The strong coherent scattering component concentrated about a narrow area called the first Fresnel zone around the specular point. As can be seen from Fig. 1, the receiver (ground-based or onboard) was equipped with two antennas: the zenith antenna is for receiving the direct RHCP signals from GPS satellite, the nadir antenna receives the reflected signals for collecting the desired surface information.

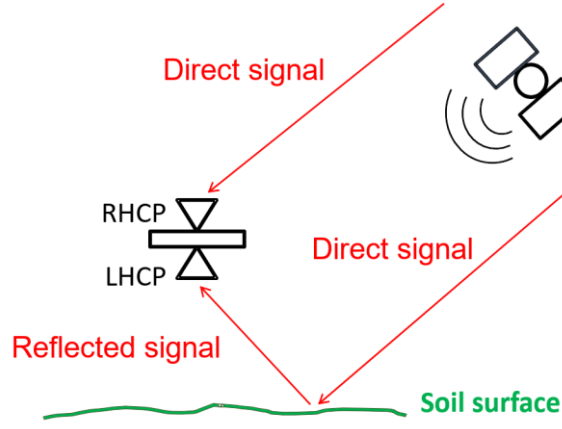


Fig. 1. Bistatic GNSS-R receiving configuration.

In this case, we can get both signal-to-noise ratio (SNR) from right-hand (RH) direct signals and left-hand (LH) reflected signals, thus the dielectric constant can be obtained from the power ratio of LH reflected SNR over direct RH SNR.

The SNR of the peak power for the direct RH signal can be written as:

$$SNR_{peak}^{direct} = \frac{P^t G^t}{4\pi R_{rt}^2} \frac{G^r \lambda^2 G_{pr}}{4\pi P_n}, \quad (2)$$

where R_{rt} represents the distance between the receiver and the transmitter. It is noted that gain G^r and noise power P_n of equipment that is given by (2) are not equal to those given by the reflected signal path, and thus a calibration is needed. By making the ratio of direct link (2) to the power equations from the reflected path, the same parameters can be canceled, and the uncertainties of G^r and P_n can be summarized into a calibration parameter C as shown:

$$\frac{SNR_{peak}^{reflect}}{SNR_{peak}^{direct}} = \frac{R_{rt}^2}{(R_{st} + R_{rs})^2} |\Gamma_{lr}| \cdot C. \quad (3)$$

Now, for the software development, input parameters of R_{rt} , R_{st} , θ (incident angle) and R_{rs} are easy to acquire from the GNSS receiver. Calibration parameter C can be either ignored if there's no way to calibrate the system or commonly can be calculated through a water measurement, since the water surface reflectivity of 0.67 is already known, the dielectric constant can be obtained from combined the Fresnel equations [13] as a numerical solution with given all the input parameters defined.

3. RESULTS

As noted previously, the SM retrieval problems can be solved by the ML methods. In this section, we will use RF to perform the regression of SM and evaluate the weight for the input variables. Hence, a simulation data set was first built for regression tasks. The input vector consists of Γ (reflectivity) and γ (elevation angle), the output vector is the SM. The simulated dataset was built by following input vectors with (3):

1. Reflectivity Γ , which ranged from 0 - 0.8
2. Elevation angle γ , which ranged from 70 degree to 85 degree

The designed range of the input data for training is aimed at covering the values ranging in common measurements. With bistatic equations (3), the simulated input vectors, and the Fresnel equations [13] of GNSS-R, the SMC can be retrieved from the dielectric constant by using a semi-empirical soil model [16]. The simulated data set were composed of 2000 points (Γ, γ, SMC) as shown in Fig. 2.

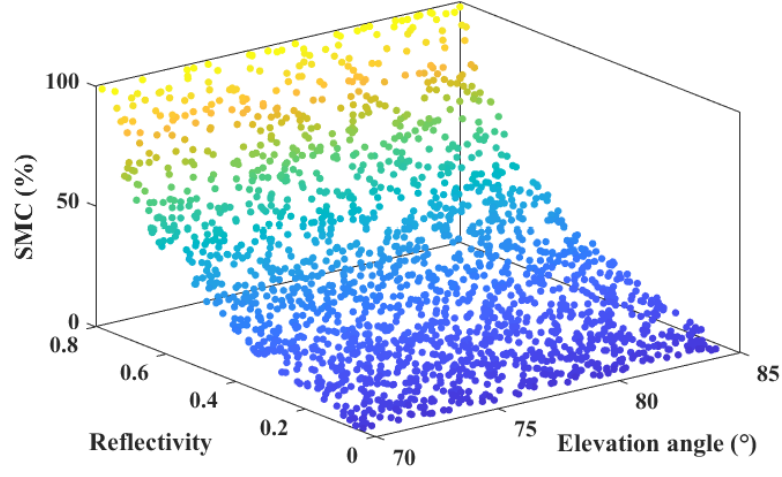
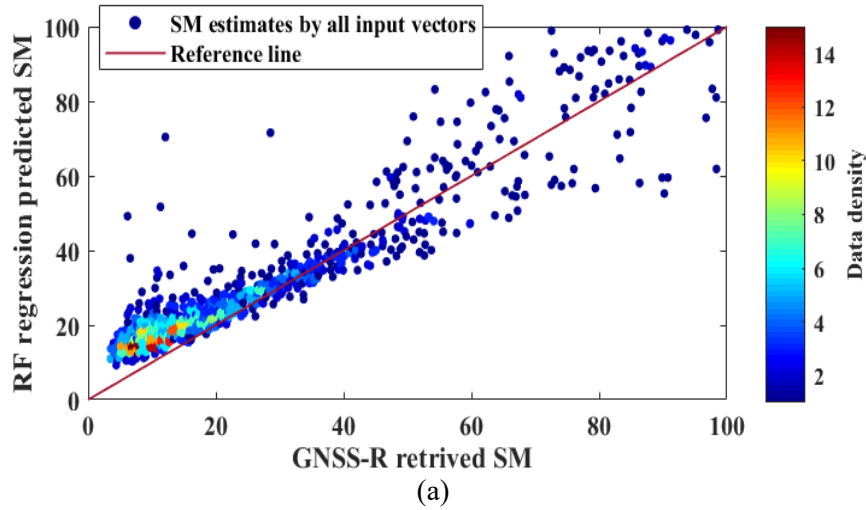


Fig. 2. The simulated data set for SM regression.

Good performance in SM regression has been demonstrated, with the applied RF methods. The output dielectric constant and SM were determined by the bistatic mode (Γ, θ). It was reported that the Γ could be the most sensitive parameter to SM in the bistatic mode [9-15]. Since the direct signal is relatively stable, the change of Γ is mainly determined by the reflected signal. It means that when only a reflected signal was received, the fluctuation of the received signal is mainly caused by the reflected SNR , and it shows the highest contribution. In this study, the RF method was selected since it showed outperformed behavior in previous studies, hence we tried to use different input parameters in RF separately to predict the SM in order to test the contributing behavior of the input vectors for SM retrieval. Here, more samples were considered for increasing the stability of the prediction, and the range of the input vector was expanded to cover as many situations as possible.

As we introduced above, the data set was simulated from dual-antenna mode to involve more input variables, and the generated simulation data including SNR, θ, SMC . Each separate independent variable and the expected value were used as a set of training and prediction data for soil moisture. Fig. 3 presents the predicted results for changing the input variables with all input variables, SNR , θ , respectively. The simulated dataset was generated by the randomization process in order to improve the reliability of the results. Each variable is used as the independent variable for random forest prediction. The statistical results are summarized in Table I. With all input vectors (3.a), the root mean square error (RMSE) is 13.3 % and the correlation coefficient $R = 0.97$. When it only has SNR vector for the input of the RF model, the RMSE is 21.35 % and the $R = 0.90$ (3.b). Fig. 3 (c) represents only the vector θ that was used for RF prediction. Its RMSE is 58.51, and the Pearson correlation coefficient $R = -0.03$.



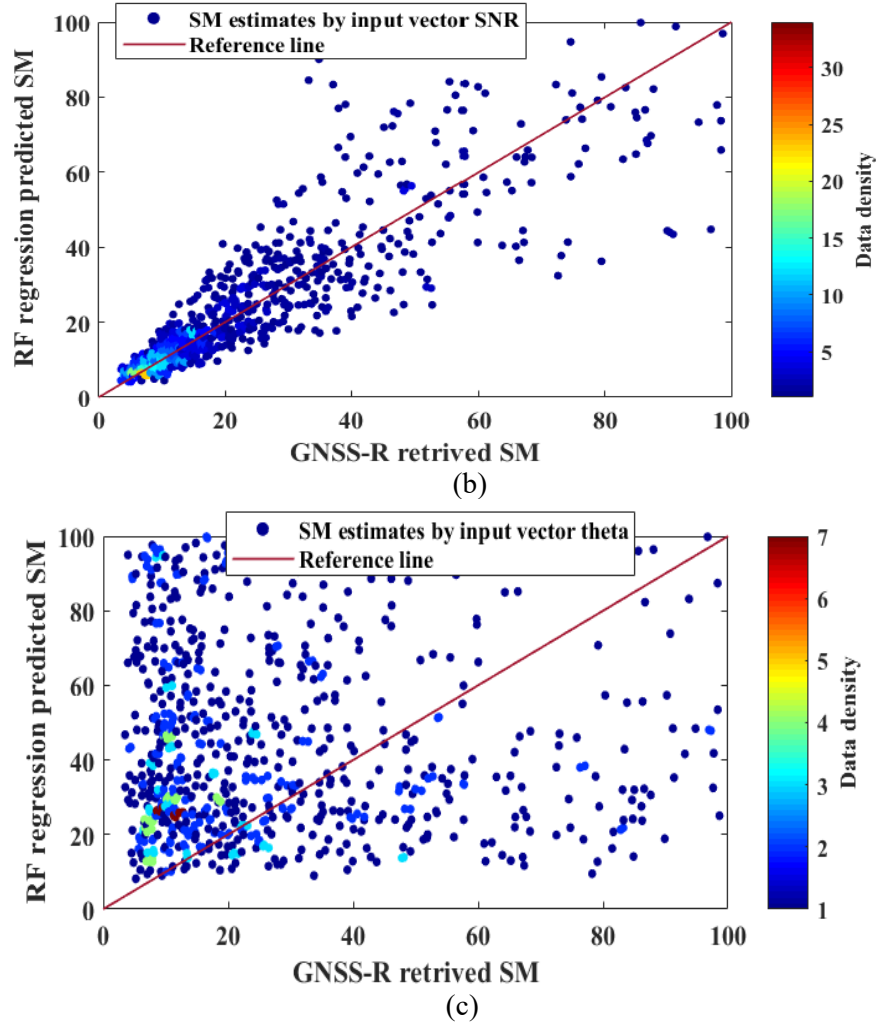


Figure 3. The weight evaluation result of RF for (a) all input variables, (b) SNR , (c) Θ .

Table I. The performance matrix of soil moisture estimation by using RF for simulated data.

Input for RF model	RMSE(%)	R
all input variables	13.35	0.97
only SNR	21.35	0.90
only Θ	58.51	-0.03

It can be seen from Fig. 3 that although the single SNR value prediction effect is not as good as the prediction using all the variables and Θ , the trend of a single SNR prediction is close to the actual value. It can also be seen from Table I that the correlation coefficient of the single SNR value prediction result reaches 90%, while the correlation coefficient of the other independent variable prediction results is about 0%, and the contribution of input SNR to the results can be considered to be the most. Therefore, it can be inferred that the input vector SNR plays the main role in the prediction of SM among the independent variables, which agrees with [17-19]. This conclusion was also proposed using the amplitude and phase of the extracted SNR observations as the independent variables for soil moisture retrieval, confirming a strong correlation between SNR and soil moisture.

4. CONCLUSION

In this study, we used machine learning methods to aid the GNSS-R soil moisture retrieval. A typical machine learning algorithm, RF was applied in GNSS-R soil moisture sensing regression. Regression results are presented with the traditional GNSS-R methods. Good predictions are obtained and the parameters of performance metrics of applied RF are analyzed. The RF showed good performance with a higher R and a smaller RMSE. Moreover, we separated input variables and compared each regression result. With all input variables, the prediction performed well; additionally, it showed that, among the dependent input variables, the variable SNR is a predominant variable that makes the most contribution to the retrieved SM, which agrees with the conclusion from [17-19].

In the learning process, it is noted in the literature that the normalization of the input vectors before the training process can speed up the convergence of the elapsed time and enhance the prediction performance. Moreover, when generating simulated data, it is necessary to shuffle the order of each dependent variable group so that the values of the dependent variable after normalization are different hence ensuring the accuracy of the training.

The study shows the prospects of using MLs to represent a complex process that is difficult to model using analytical approaches. The ML methods can help to reveal the complex interactions between inputs and outputs, meanwhile making good predictions. Thus, they could be used as an alternative to the complex and data-intensive retrieval process and are applicable in various situations. This study helps to understand the internal relationships between inputs and outputs, and provides some experimental insights into the behavior of the GNSS-R soil moisture retrieval procedure which can benefit various diverse research areas.

REFERENCES

1. J. Darrozes, N. Roussel, M. Zribi, "The reflected Global Navigation Satellite System (GNSS-R): from theory to practice," in *Microwave Remote Sensing of Land Surface*, Elsevier, pp. 303-355, 2016.
2. M. C. Dobson and F. T. Ulaby, "Active microwave soil moisture research," *IEEE Trans. Geosci. Remote Sens.*, no. 1, pp. 23-36, 1986.
3. M. Martin-Neira, "A passive reflectometry and interferometry system (PARIS): Application to ocean altimetry," *ESA J.*, vol. 17, pp. 331-355, 1993.
4. J. L. Garrison, S. J. Katzberg, M. I. Hill, "Effect of sea roughness on bistatically scattered range coded signals from the global positioning system," *Geophys. Res. Lett.*, vol. 25, pp. 2257-2260, 1998.
5. V. U. Zavorotny, A. G. Voronovich, "Scattering of GPS signals from the ocean with wind remote sensing application," *IEEE Trans. Geosci. Remote Sens.*, vol. 38, no. 2, pp. 951-964, Mar. 2000.
6. S. T. Lowe, P. M. Kroger, G. W. Franklin, J. L. LaBrecque, J. Lerma, M. F. Lough, M. R. Marcin, D. J. Spitzmesser, L. E. Young, "A delay/Doppler-mapping receiver system for GPS-reflection remote sensing," *IEEE Trans. Geosci. Remote Sensing*, vol. 40, no. 5, pp. 1150-1163, 2002.
7. J. F. Marchan-Hernandez, N. Rodriguez-Ivarez, A. Camps, X. Bosch-Lluis, I. Ramos-Perez, "Correction of the sea state impact in the L-band brightness temperature by means of delay-Doppler maps of global navigation satellite signals reflected over the sea surface," *IEEE Trans. Geosci. Remote Sens.*, vol. 46, no. 10, pp. 2914-2923, Oct. 2007.
8. D. Masters, P. Axelrad, S. Katzberg, "Initial results of land-reflected GPS bistatic radar measurements in SMEX02," *Remote Sens. Environ.*, vol. 92, no. 4, pp. 507-520, 2002.
9. S. Katzberg, O. Torres, M. Grant, D. Masters, "Utilizing calibrated GPS reflected signals to estimate oil reflectivity and dielectric constant: Results from SMEX02," *Remote Sens. Environ.*, vol. 100, no. 1, pp. 17-28, 2006.
10. D. Masters, A. Penina, and S. Katzberg, "Initial results of land-reflected GPS bistatic radar measurements in SMEX02," *Remote Sens. Environ.*, vol. 92, no. 4, pp. 507-520, 2004.
11. A. Egido, M. Caparrini, G. Ruffini, S. Paloscia, E. Santi, L. Guerriero, N. Pierdicca, and N. Floury, "Global navigation satellite systems reflectometry as a remote sensing tool for agriculture," *Remote Sens.*, vol. 4, no. 8, pp. 2356-2372, 2012..
12. V. U. Zavorotny, K. M. Larson, J. J. Braun, E. E. Small, E. D. Gutmann, A. L. Bilich, "A physical model of GPS multipath caused by land reflections: Toward bare soil moisture retrievals," *IEEE J. Sel. Topics Appl. Earth Obs. Remote Sens.*, vol. 3, no. 1, 2009.
13. Y. Jia, P. Savi, D. Canone, & R. Notarpietro, "Estimation of Surface Characteristics Using GNSS LH-Reflected Signals: Land Versus Water," *IEEE Journal of Selected Topics in Applied Earth Observations and Remote Sensing*, vol. 9, no. 10, pp. 4752-4758, 2016.
14. K. M. Larson, J. J. Braun, E. E. Small, V. U. Zavorotny, E. D. Gutmann, and A. L. Bilich, "GPS multipath and its relation to near- surface soil moisture content," *IEEE J. Sel. Top. Appl. Earth Obs. Remote Sens.*, vol. 3, no. 1, pp. 91-99, Mar. 2010.
15. Q. Yan, W. Huang, S. Jin, & Y. Jia, "Pan-tropical soil moisture mapping based on a three-layer model from CYGNSS GNSS-R data," *Remote Sensing of Environment*, vol. 247, pp. 111944, 2020.
16. C. M. Dobson, T. F. Ulaby, T. M. Hallikainen, et al, "Microwave dielectric behavior of wet soil-Part II: Dielectric mixing models," *IEEE Transactions on Geoscience and Remote Sensing*, vol. 1, pp. 35-46, 1985.
17. A. Camps, H. Park, M. Pablos, G. Foti, C. P. Gommenginger, & P. W. Liu, et al. "Sensitivity of gnss-r spaceborne observations to soil moisture and vegetation," *IEEE Journal of Selected Topics in Applied Earth Observations & Remote Sensing*, vol. 9, no. 10, pp. 4730-4742, 2016.
18. H. Carreno-Luengo, G. Luzi, & M. Crosetto, "Sensitivity of cygnss bistatic reflectivity and smap microwave radiometry brightness temperature to geophysical parameters over land surfaces," *IEEE Journal of Selected Topics in Applied Earth Observations and Remote Sensing*, vol. 12, no. 1, pp. 107-122, 2019.
19. N. Rodríguez-Fernández, A. Al Bitar, A. Colliander, & T. Zhao, "Soil moisture remote sensing across scales," *Remote Sensing*, vol. 11, no. 2, pp. 190-194, 2019.